

# Evidence for two superconducting components in oxygen-annealed single-phase Y-Ba-Cu-O\*

R.B. Goldfarb, A.F. Clark, A.I. Braginski<sup>†</sup> and A.J. Panson<sup>†</sup>

Electromagnetic Technology Division, National Bureau of Standards,  
Boulder, CO 80303, USA

<sup>†</sup>Research and Development Center, Westinghouse Electric Corporation,  
Pittsburgh, PA 15235, USA

Received 8 June 1987

The complex susceptibility of a sintered Y-Ba-Cu-O superconductor is strongly dependent on a.c. field amplitude,  $h$ . Very small values of  $h$  must be used for the real part of susceptibility,  $\chi'$ , to reach a value corresponding to bulk diamagnetism just below the critical temperature,  $T_c$ . The imaginary part,  $\chi''$ , represents hysteresis loss in the sample. Thus,  $\chi''$  versus temperature becomes positive when  $h$  exceeds the lower critical field,  $H_{cl}$ , of the superconductor.

Annealing the material in oxygen gives rise to two distinct components, a relatively high- $T_c$ , high- $H_{cl}$  superconductor (denoted as 'G' or 'good') and a relatively low- $T_c$ , low- $H_{cl}$  superconductor (denoted as 'B' or 'bad'). Curves of susceptibility versus increasing temperature reflect the dual nature of the annealed sample:  $\chi'$  has an inflection point at  $T_c$  of the B component and approaches zero at  $T_c$  of the G component, while  $\chi''$  has a peak at each  $T_c$ . Both critical temperatures decrease linearly with increasing  $h$ , though at very different rates.  $H_{cl}$  of the G component is considerably greater than  $H_{cl}$  of the B component. The lower critical fields are linearly decreasing functions of temperature.

Two models might explain the susceptibility data. In the grain model, the G component consists of superconducting grains and the B component is either intergranular material, unfavourably orientated anisotropic grains, or oxygen-depleted grain boundaries. In the surface model, the G component is in the interior of the sample and the B component is at the sample's surface. This condition could arise if there was oxygen depletion at the surface subsequent to total enrichment during annealing.

**Keywords:** superconductors; Y-Ba-Cu-O superconductors; high critical temperature superconductors; a.c. losses; susceptibility; lower critical field

The measurement of a.c. susceptibility,  $\chi$ , as a function of temperature,  $T$ , is often used to determine the critical temperature,  $T_c$ , of superconductors<sup>1,2</sup>. In general, the real part of susceptibility,  $\chi'$ , goes from  $-1$  (SI units) below  $T_c$ , indicating perfect diamagnetism and flux shielding, to a small positive value above  $T_c$ , indicating the normal paramagnetic state. The imaginary (loss) part of susceptibility,  $\chi''$ , goes from zero below  $T_c$ , through a peak near  $T_c$ , to zero in the normal state.

The derivative of the initial curve of magnetization versus magnetic field is volume susceptibility. For a large enough field amplitude, hysteresis loss will appear as an enclosed area in the magnetization-field plane. In such a state, the material is not perfectly diamagnetic,  $\chi''$  is greater than zero, and  $\chi'$  is no longer equal to  $-1$ .

We examine  $\chi'$  and  $\chi''$  as functions of  $T$  for different values of a.c. field amplitude,  $h$ , and frequency,  $f$ , for a high- $T_c$ , sintered, X-ray single-phase, copper-oxide superconductor,  $Y_1Ba_2Cu_3O_{8-\delta}$ , where  $\delta$  represents an unknown oxygen deficiency. The character of the  $\chi$  curves changes significantly after annealing the sintered material in oxygen. The curves indicate a transformation of the original material into two distinct superconducting components. From the  $\chi$  curves we deduce  $T_c(h)$  and  $H_{cl}(T)$  for each component, where  $H_{cl}$  is the lower critical field. One component, with relatively high  $T_c$  and  $H_{cl}$ , is denoted as 'G' or 'good'. The other, with relatively low  $T_c$  and  $H_{cl}$ , is denoted as 'B' or 'bad'.

Two physical models are consistent with the susceptibility data. In the grain model, the G component is identified as superconducting grains and the B component is either intergranular material, unfavourably orientated anisotropic grains, or oxygen-depleted grain boundaries. The two components are dispersed throughout the sample. In the surface model, the G component is

\*Paper presented at CEC/ICMC, St Charles, Illinois, USA, 14-18 June 1987. Contribution of the National Bureau of Standards, not subject to copyright

located in the interior of the sample and the B component is the region at the sample's surface.

In conventional 'hard' type-II superconductors, the lower critical field,  $H_{c1}$ , corresponds to the field above which: 1, magnetic flux penetrates into the superconductor and is subjected to pinning forces; 2, hysteresis loss appears; and 3, the curve of magnetization *versus* field deviates from linearity\*. Therefore, when the  $h$  used in a susceptibility measurement exceeds  $H_{c1}$ , positive  $\chi''$  is expected<sup>4</sup>. (If necessary, the value of  $h$  should be corrected for the sample demagnetization factor.) Thus, measurements of  $\chi''$  *versus*  $T$  for different values of  $h$  may be used to deduce  $H_{c1}(T)$ <sup>†</sup>.  $H_{c1}$  is sometimes difficult to obtain from curves of magnetization *versus* field because deviation from linearity is often not readily apparent.

In granular superconductors, superconducting grains may be coupled via Josephson currents through insulating barriers (tunneling) or normal-metal junctions (proximity effect)<sup>6-8</sup>. Since this description might apply to Y-Ba-Cu-O superconductors<sup>9-13</sup>, one would distinguish between the lower critical field of the grains and the significantly smaller 'Josephson lower critical field'<sup>14</sup>. In this model, the definition of  $H_{c1}$  above would apply to the Josephson lower critical field rather than the superconducting grains. In variations of the grain model, the definition of  $H_{c1}$  would apply to either unfavourably orientated anisotropic grains<sup>15-17</sup> or to oxygen-depleted grain boundaries.

In the surface model, the region near the sample surface is simply a B superconductor, not Josephson material.  $H_{c1}$  in the traditional definition above would apply to the surface region, not the G interior. In any case, we use the symbols  $T_{cg}$  and  $H_{c1g}$  to refer to  $T_c$  and  $H_{c1}$  of the G superconductor. Similarly, we use  $T_{cb}$  and  $H_{c1b}$  to refer to  $T_c$  and  $H_{c1}$  of the B material.

## Experimental details

The  $Y_1Ba_2Cu_3O_{8-\delta}$  superconductor was fabricated as described by Panson *et al.*<sup>18</sup>. If  $\delta$  were equal to zero, it would imply that all Cu was in the trivalent state. For  $\delta$  greater than zero, some Cu is divalent. The pressed powder was sintered at 940°C and cooled in oxygen. The material is single-phase orthorhombic as determined by X-ray diffraction. Grain size is of the order of 10  $\mu\text{m}$ . Prior to measurement, the two large sample surfaces were sanded to remove surface contamination and to ensure flat faces. After measuring  $\chi$  for different  $h$  and  $f$ , the same sample was annealed in flowing oxygen at ambient pressure ( $\approx 80$  kPa) at 700°C for  $\approx 40$  h and slowly furnace cooled to room temperature. It took 2 h for the

temperature to fall from 700 to 350°C. Samples so prepared are crystallographically single phase within the resolution of X-ray diffraction<sup>18</sup>. After annealing the sample,  $\chi$  was again measured. Between measurements the sample was stored in a desiccator.

A proper combination of sample dimensions and maximum  $f$ , appropriate to the normal-state residual resistivity, eliminates normal-state eddy-current effects near  $T_c$ . Intergranular residual resistivity is 350–400  $\mu\Omega$  cm. The normal-state skin depth at 1000 Hz is  $\approx 3$  cm, compared to a sample thickness of  $\approx 1$  mm. Thus, in this sample,  $\chi''$  represents only hysteresis loss. However, if sample dimensions perpendicular to the applied field were large and normal-state resistivity were low enough, eddy currents could contribute to  $\chi$  near  $T_c$ .

Volume susceptibility was measured with an a.c. susceptometer calibrated, for these measurements, with a Nb sphere at 4 K<sup>19</sup>. (Normal-state eddy-current effects would not be seen this far below  $T_c$  of  $\approx 9.6$  K.) The susceptibility values reported are thus accurate to the extent that the sample moment approximates a dipole. The sample used for the susceptibility measurements was a thin, flat piece with  $h$  applied in the plane. Sample dimensions were  $\approx 12 \times 7.2 \times 0.9$  mm, with an estimated<sup>20</sup> effective demagnetization factor of 0.05. External susceptibilities, not corrected for this small demagnetization factor, are presented in the results. The overall sample volume, including voids, was used to compute  $\chi$ . Sample density was 4.8 g cm<sup>-3</sup>. Based on a comparison to the 5.3 g cm<sup>-3</sup> pycnometric density of the powder, 10% of the sample volume would be voids. Based on an ideal 6.4 g cm<sup>-3</sup> X-ray density, 25% of the sample volume would be voids.

A high-permeability shield around the Dewar reduced the Earth's field to less than 0.4 A m<sup>-1</sup> (5 mOe) in the measurement axis. The sample was cooled to either 4 or 76 K in zero magnetic field. Measurements were made with  $T$  increasing at the rate of 0.2 K min<sup>-1</sup> or less. As  $T$  increased,  $f$  was cycled between 10, 100 and 1000 Hz. Hence, each measurement run yielded  $\chi$  curves for three frequencies at constant  $h$ . The phase angle of the lock-in amplifier used in the experiment was determined for each measurement frequency to null  $\chi''$  for a small  $h$  at 4 K.

## Results and discussion

### Unannealed sample

Both  $\chi'$  and  $\chi''$  for the unannealed sample are plotted from 75 to 95 K in Figure 1 for a range of  $h$  at 100 Hz. The curves are labelled with numbers equal to the r.m.s. measuring field in Oe. The transition from the normal to the superconducting state begins at 90 K, but the shapes of the  $\chi$  curves are strongly dependent on  $h$ . In fact, very small values of  $h$  must be used for  $\chi'$  to reach  $-1$  just below  $T_c$  and for the apparent width of the transition to be small. For the smallest  $h$ , the transition width is 3 K, similar to that measured resistively. Most papers reporting susceptibility of high- $T_c$  copper-oxide superconductors either present  $\chi$  values in arbitrary units or report measurements made in applied fields that are too large for perfect diamagnetism to be seen just below  $T_c$ . There are some exceptions<sup>4,21-24</sup>.

As  $h$  increases, the character of the  $\chi'$  and  $\chi''$  curves changes. The  $\chi''$  curve goes from having a peak to having a

\*In an ideal type-II superconductor, assuming zero demagnetization factor and thus no intermediate state, the field of maximum (negative) magnetization also coincides with  $H_{c1}$ . However, in hard type-II superconductors, those characterized by flux pinning, it corresponds to the 'full-penetration' field at which flux lines first penetrate to the centre of the superconductor in the mixed state. For higher fields, the critical current density, and therefore the magnetization, decrease in magnitude<sup>3</sup>.

<sup>†</sup>An alternate, but conceptually equivalent, method to obtain  $H_{c1}$  from  $\chi''$  is to measure low-field a.c.  $\chi$  in a variable d.c. bias field<sup>9</sup>. In such an experiment we observe features in the  $\chi$  curves that are the same as those we report here. There is not, however, a perfect correlation between the magnitudes of the d.c. bias field and  $h$ .

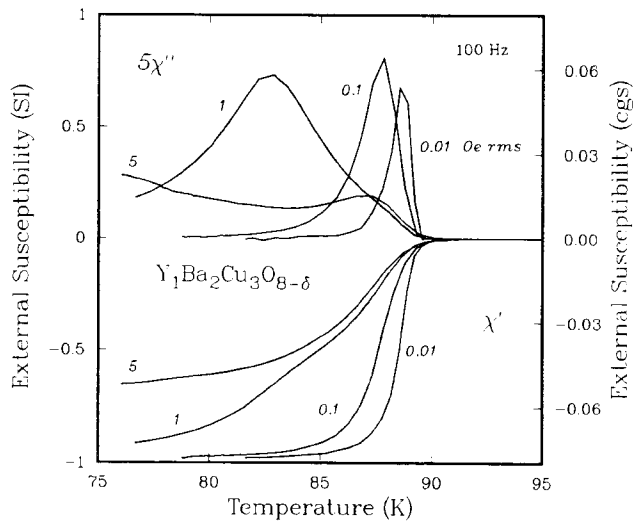


**Figure 1** Real ( $\chi'$ ) and imaginary ( $\chi''$ ) susceptibility for sintered but unannealed  $\text{Y}_1\text{Ba}_2\text{Cu}_3\text{O}_{8-\delta}$ . The numbers labelling the curves are the r.m.s. values of the measuring fields in Oe. Measurements were made for field amplitudes,  $h$ , of  $1.1 \text{ A m}^{-1}$  (14 mOe) [curves 0.01],  $11 \text{ A m}^{-1}$  (0.14 Oe) [curves 0.1],  $113 \text{ A m}^{-1}$  (1.4 Oe) [curves 1] and  $563 \text{ A m}^{-1}$  (7 Oe) [curves 5]. Each curve is composed of straight-line segments connecting about 30 data points. For purposes of clarity,  $\chi''$  is multiplied by 5 and only data for 100 Hz are shown. Curves for  $f$  of 10 and 1000 Hz are virtually identical. (After Reference 4)

broad maximum. For the highest field, the maximum of  $\chi''$  is below 75 K and a secondary peak appears near 87 K. When  $h$  exceeds the lower critical field,  $H_{c1}$ , of the superconductor at a given temperature below  $T_c$ ,  $\chi''$  becomes positive and  $\chi'$  is no longer equal to  $-1$ . Thus, measurements of  $\chi$  as a function of  $T$  allow  $H_{c1}(T)$  to be determined, as shown in more detail for the annealed sample below. For a field amplitude,  $h$ , equal to  $1.1 \text{ A m}^{-1}$  (14 mOe) [curves 0.01],  $\chi''$  first becomes positive upon warming at 87 K, indicating  $H_{c1}(87) = 1.1 \text{ A m}^{-1}$ . By the same logic,  $H_{c1}(85) = 11 \text{ A m}^{-1}$  (0.14 Oe) [curves 0.1]. Because  $H_{c1}$  is extremely small for the unannealed material, even moderate values of  $h$  prevent  $\chi'$  from reaching  $-1$  below  $T_c$ .

#### Annealed sample

Susceptibility data for the sample after annealing at  $700^\circ\text{C}$  for  $\approx 40 \text{ h}$  are plotted in Figure 2 for field amplitude,  $h$ , equal to  $225 \text{ A m}^{-1}$  (2.8 Oe) at  $f$  of 10, 100 and 1000 Hz. The data illustrate that  $\chi$  is independent of  $f$ . This value of  $h$  was selected because there are very distinguishable features in  $\chi'$  and  $\chi''$  which we interpret as corresponding to two superconducting components in the material. Peaks in  $\chi''$  and inflection points in  $\chi'$  denote their critical temperatures. The critical temperature of the B material,  $T_{cb}$ , is  $\approx 86.8 \text{ K}$  and the critical temperature of the G material,  $T_{cg}$ , is  $\approx 91.3 \text{ K}$ . These temperatures correspond to approximately the midpoints of the transitions.

Data for a full range of  $h$  at 100 Hz are plotted in Figure 3. The curves are labelled with numbers equal to the r.m.s. measuring field in Oe. For a very small field amplitude,  $h$ , of  $1.1 \text{ A m}^{-1}$  (14 mOe) [curves 0.01], a single sharp transition is seen at 91 K, with a transition width of  $\approx 2 \text{ K}$ . For a larger  $h$  of  $11 \text{ A m}^{-1}$  (0.14 Oe) [curves 0.1],  $T_c$  moves to lower temperature and the transition width broadens. For  $h$  equal to or greater than  $113 \text{ A m}^{-1}$

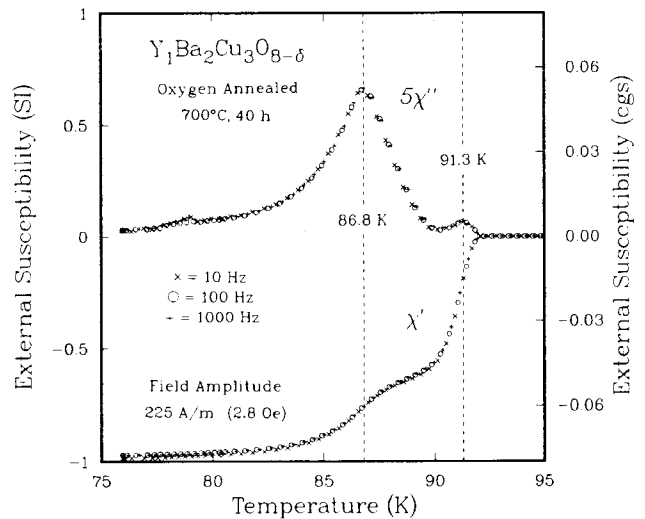


**Figure 2** Real ( $\chi'$ ) and imaginary ( $\chi''$ ) susceptibility illustrating the two-component nature of  $\text{Y}_1\text{Ba}_2\text{Cu}_3\text{O}_{8-\delta}$  annealed in oxygen at ambient pressure at  $700^\circ\text{C}$  for 40 h. Measurements are shown for a field amplitude,  $h$ , of  $225 \text{ A m}^{-1}$  (2.8 Oe) at frequencies,  $f$ , of 10 Hz (x), 100 Hz (O) and 1000 Hz (+). Susceptibility is virtually independent of  $f$ . For purposes of clarity,  $\chi''$  is multiplied by 5. The peaks in  $\chi''$  coincide with approximately the temperatures of the midpoints of the transitions in  $\chi'$  for each component

(1.4 Oe) [curves 1–10], the presence of the two superconducting components is apparent. The  $\chi''$  curves have double peaks and the  $\chi'$  curves have two fall-offs.

The critical temperatures,  $T_{cg}$  and  $T_{cb}$ , of the two components are shown in Figure 4 as functions of  $h$ . With increasing  $h$ , the critical temperatures decrease linearly but at unequal rates. The slope  $dT_{cb}/dh$  is 50 times  $dT_{cg}/dh$ . The plotted values were determined from the peak

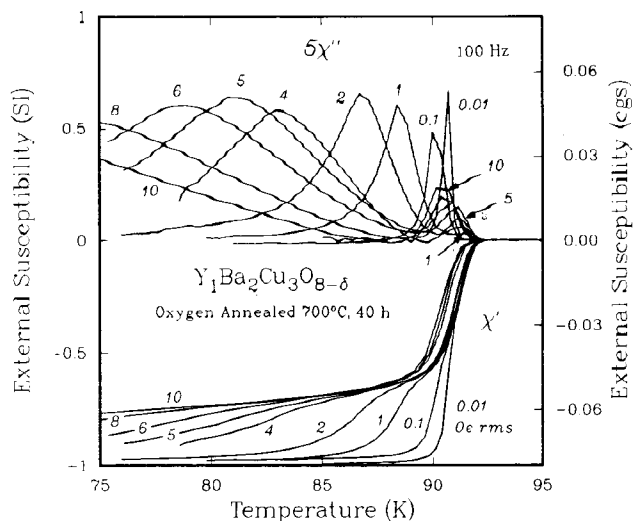


**Figure 3** Real ( $\chi'$ ) and imaginary ( $\chi''$ ) susceptibility for oxygen-annealed  $\text{Y}_1\text{Ba}_2\text{Cu}_3\text{O}_{8-\delta}$ . The numbers labelling the curves are the r.m.s. values of the measuring fields in Oe. Measurements were made for field amplitudes,  $h$ , of  $1.1 \text{ A m}^{-1}$  (14 mOe) [curves 0.01],  $11 \text{ A m}^{-1}$  (0.14 Oe) [curves 0.1],  $113 \text{ A m}^{-1}$  (1.4 Oe) [curves 1],  $225 \text{ A m}^{-1}$  (2.8 Oe) [curves 2, seen also in Figure 2],  $450 \text{ A m}^{-1}$  (5.7 Oe) [curves 4],  $563 \text{ A m}^{-1}$  (7.1 Oe) [curves 5],  $675 \text{ A m}^{-1}$  (8.5 Oe) [curves 6],  $900 \text{ A m}^{-1}$  (11.3 Oe) [curves 8] and  $1125 \text{ A m}^{-1}$  (14.1 Oe) [curves 10].  $\chi''$  curves [1]–[10] have double peaks. Each curve is composed of straight-line segments connecting about 40 data points. For purposes of clarity,  $\chi''$  is multiplied by 5 and only data for 100 Hz are shown. Curves for frequencies of 10 and 1000 Hz are virtually identical

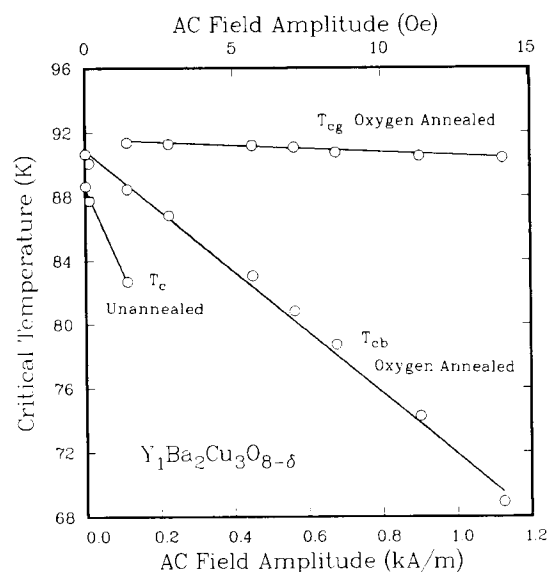


**Figure 4** Critical temperatures,  $T_{cg}$  and  $T_{cb}$ , of the two superconducting components in  $Y_1Ba_2Cu_3O_{8-\delta}$  (oxygen-annealed at 700°C for 40 h) as functions of a.c. field amplitude,  $h$ . For comparison,  $T_c$  for the unannealed sample is also shown. The critical temperatures were determined by the peaks in  $\chi'$ , which correspond to approximately the midpoints of the transitions in  $\chi'$ , for each component

temperatures in  $\chi''$ , interpolated by fitting a parabola to the three highest-valued  $\chi''$  data points. For the two smallest  $h$  values,  $T_{cg}$  cannot be found from  $\chi''$  because there is no second peak. In this limit of small  $h$ ,  $T_{cg}$  and  $T_{cb}$  converge. Also plotted in Figure 4, for comparison, are  $T_c$  values for the unannealed sample. The decrease in  $T_{cb}$  with increasing  $h$  is consistent with the rapid decrease in transport critical current observed in applied fields in the range 80–8000 A m<sup>-1</sup> (1 to 100 Oe) at liquid nitrogen temperature<sup>10</sup>.

### Lower critical fields

Because  $H_{clg}$  is significantly greater than  $H_{clb}$ , larger  $h$  is required to bring out the features in  $\chi$  corresponding to flux penetration into the G component. Above  $T_{cb}$ , only the G superconductor contributes to  $\chi$ . That is why, for  $h$  less than  $H_{clg}$ , all  $\chi'$  curves merge near  $T_{cg}$  in Figure 3.

In general,  $H_{cl}$  is expected to be a decreasing function of  $T$ . Ginzburg-Landau theory, for example, shows that  $H_{cl}$  is proportional to  $1 - T/T_c$  near  $T_c^*$ . Consequently, there will be some value of  $T$  upon warming at which  $H_{cl}$  falls below  $h$ . At this  $T$ ,  $\chi''$  will begin to rise from zero. As  $T$  increases,  $H_{cl}$  continues to decrease and  $\chi''$  continues to increase. As  $T_c$  is approached, the magnetization curve collapses and both  $\chi'$  and  $\chi''$  approach zero.

The sequence of measurements using different  $h$  in Figure 3 may be used to deduce  $H_{cl}(T)$  for the two components.  $H_{clg}$  and  $H_{clb}$  are plotted versus  $T$  in Figure 5. The functions are linear, although there is some uncertainty in  $H_{clb}$  at the lower temperatures.  $H_{clg}$  is considerably greater than  $H_{clb}$  and decreases steeply with

increasing  $T$  near  $T_{cg}$  with a slope,  $dH_{clg}/dT$ , of  $-289$  A m<sup>-1</sup> K<sup>-1</sup> ( $-3.6$  Oe K<sup>-1</sup>).

### Identification of components

Because the annealing and slow cooling procedure is believed to yield material that is crystallographically single phase, we refer to the G and B superconductors as 'components', not 'phases'. The possibility that the G component is at the sample surface should be considered. This condition could exist if there was inadequate oxygen diffusion into the sample during annealing. If the G material were at the surface, however, it would effectively shield the B interior material. The latter would not be evident in the  $\chi$  curves for any  $T$  or  $h$ .

We examine two other models. In the grain model, the two components are distributed throughout the sample as grains plus either intergranular material, anisotropic grains misaligned with the field, or oxygen-depleted grain boundaries. The intergranular material could be Josephson weak links or simply B superconductor. The misaligned grains might exhibit weak superconductivity due to crystalline anisotropy such as anisotropy in the superconductive energy gap. When  $h$  is small,  $\chi'$  is characteristic of a bulk superconductor. For medium  $h$ , greater than  $H_{clb}$ , the grains decouple and  $\chi'$  decreases in magnitude to a value corresponding to a collection of decoupled grains<sup>14</sup>. For large  $h$ , greater than  $H_{clg}$ , the grains are penetrated by magnetic flux and  $\chi'$  is reduced in magnitude. These effects may be seen in Figure 3 at appropriate temperatures, since  $H_{clb}$  and  $H_{clg}$  are functions of  $T$ .

In the surface model, the G material is in the interior of the sample and B superconductor, not Josephson material, is a surface sheath. The G superconductor would contain grains and voids, but the material would be contiguous. This condition could arise from oxygen depletion at the surface subsequent to total oxygen enrichment during annealing. The depletion could be a

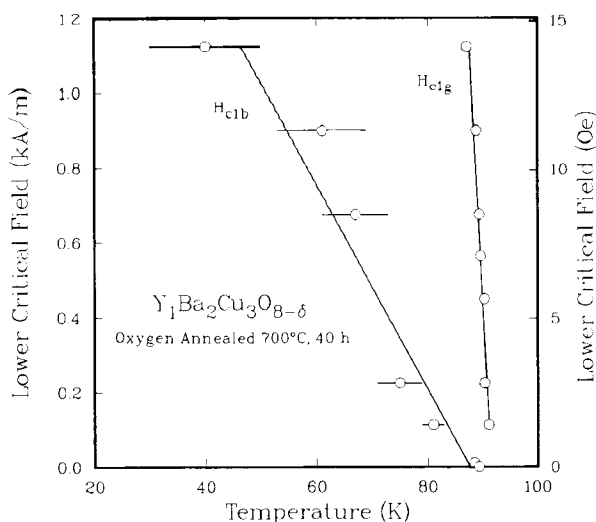


**Figure 5** Lower critical fields,  $H_{clg}$  and  $H_{clb}$ , of the two superconducting components in oxygen-annealed  $Y_1Ba_2Cu_3O_{8-\delta}$  as functions of temperature. The data were determined by the temperatures at which curves of  $\chi''$ , most shown in Figure 3, rise from zero upon warming. The gradual rise in  $\chi''$  at lower temperatures gives some uncertainty in  $H_{clb}$ , indicated by error bars. Each line is a least-squares fit with  $H_{cl}$  as the independent variable

\*This may be deduced from the theoretical expression for  $H_{cl}$  in terms of the penetration depth and the coherence length<sup>25</sup>, both functions of temperature<sup>26</sup>

consequence of reaction with water or carbon dioxide. When  $h$  is small,  $\chi'$  is once again characteristic of a bulk superconductor. When  $h$  exceeds  $H_{clb}$ , flux penetrates through the surface region until it reaches the G superconductor in the interior. When  $h$  exceeds  $H_{clg}$ , flux penetrates into the G material and  $\chi'$  is reduced in magnitude.

We have seen susceptibility evidence of two superconducting components in other samples of Y-Ba-Cu-O and La-Sr-Cu-O made at different laboratories. Others have reported similar evidence<sup>23,24</sup>. Thus the two-component phenomenon appears to occur generally, as a consequence of current methods of materials preparation and oxygen annealing. Different methods might minimize the fraction of B material.

The relative volumes of the two components may be estimated from the value of  $\chi'$  above  $T_{cb}$ . For example, in Figure 2, we assume that the G component is perfectly diamagnetic at 89 K and that the B material does not contribute to  $\chi'$  for this  $T$  and  $h$ . Then  $\chi'$  is entirely due to the G material. If  $\chi'$  is  $\approx 0.65$  (SI), then 65% of the volume is occupied by G material. In the grain model, if the grains are large enough to avoid penetration-depth effects<sup>14</sup>, the remainder of the volume is composed of B material and voids. In the surface model, the remainder of the volume is B material and the voids are distributed uniformly throughout the sample.

## Conclusions

The critical temperature,  $T_c$ , of unannealed, X-ray single phase, sintered  $Y_1Ba_2Cu_3O_{8-\delta}$  is relatively low and decreases rapidly with increasing a.c. field amplitude,  $h$ . The lower critical field,  $H_{cl}$ , is quite small.

Annealing the sample in oxygen and slowly cooling preserves the single crystallographic phase, but gives rise to two superconducting components. The components are identified as 'good' ('G') and 'bad' ('B') superconducting material, with critical temperatures  $T_{cg}$  and  $T_{cb}$ . The dual nature of the annealed sample is clearly evident in curves of complex susceptibility,  $\chi$ , versus increasing temperature,  $T$ :  $\chi'$  has an inflection point at  $T_{cb}$  and approaches zero at  $T_{cg}$ .  $\chi''$  has a peak corresponding to each  $T_c$ . Both critical temperatures decrease linearly with  $h$ , but at very different rates. For all  $h$ ,  $T_{cg}$  is greater than  $T_{cb}$  which, in turn, is greater than  $T_c$  of the unannealed superconductor.

The lower critical fields of the two components,  $H_{clg}$  and  $H_{clb}$ , are linearly decreasing functions of  $T$ .  $H_{clg}$  is much greater than  $H_{clb}$  and  $H_{cl}$  of the unannealed superconductor. The G component appears to be much better superconductor than the B component based on the data for  $T_c(h)$  and  $H_{cl}(T)$ . At temperatures greater than  $T_{cb}(h)$ , there is a reduction in the effective volume of superconductor and in the magnitude of  $\chi'$ .

## Added in proof

In order to possibly increase the oxygen content of the sample and, in particular, that of the B component, we reannealed the sample in flowing oxygen according to the following schedule: 650°C/2 h, 450°C/24 h, 400°C/24 h, 350°C/16 h, slow cool to room temperature. Susceptibility versus temperature was measured with  $h$  equal to

225 A m<sup>-1</sup> (2.8 Oe) at 100 Hz for comparison with Figure 2. The low-temperature  $\chi''$  peak associated with  $T_{cb}$  shifted slightly upward to 87.3 K. The upper-temperature  $\chi''$  peak and the fall-off in  $\chi'$  corresponding to  $T_{cg}$  both shifted slightly downward to 91.0 K. The magnitudes of the peaks remained about the same. Based on these results, oxygen deficiency might not be a factor for the B component.

## Acknowledgements

We had helpful discussions with J.W. Ekin, L.F. Goodrich and J. Moreland. The a.c. susceptometer was constructed by C.A. Thompson. Y. Melchizedek and D.L. Ried assisted with computer programming and data reduction. Comparison samples of Y-Ba-Cu-O were generously provided by M. Hong, AT&T Bell Laboratories, and by J. E. Blendell, National Bureau of Standards. Comparison samples of La-Sr-Cu-O were generously provided by H.C. Ku and R.N. Shelton, Iowa State University. Work at NBS was supported by the National Engineering Laboratory, National Bureau of Standards. Work at Westinghouse was supported in part by the Air Force Office of Scientific Research, USA, contract No. F49620-85-C-0043.

## References

- 1 Maxwell, E. and Strongin, M. Filamentary structure in superconductors *Phys Rev Lett* (1963) **10** 212
- 2 Hein, R.A. AC magnetic susceptibility, Meissner effect and bulk superconductivity *Phys Rev B* (1986) **33** 7539
- 3 Carr, Jr., W.J. *AC Loss and Macroscopic Theory of Superconductors* Gordon and Breach, New York, USA (1983) 16-19
- 4 Goldfarb, R.B., Clark, A.F., Panson, A.J. and Braginski, A.I. AC susceptibility measurements near the critical temperature of a Y-Ba-Cu-O superconductor, in: *High Temperature Superconductors* (Eds Gubser, D.U. and Schluter, M.) Materials Research Society, Pittsburgh, USA (1987) EA-11 261
- 5 Finnemore, D.K. Personal communication, Iowa State University, USA (1987)
- 6 Bastuscheck, C.M., Buhrman, R.A. and Scott, J.C. Magnetic behavior of a superconductor-normal-conductor composite (SN)<sub>x</sub> *Phys Rev B* (1981) **24** 6707
- 7 Ebner, C. and Stroud, D. Diamagnetic susceptibility of superconducting clusters: spin-glass behavior *Phys Rev B* (1985) **31** 165
- 8 England, P., Goldie, F. and Caplin, A.D. Electrical transport and magnetisation measurements on a 3D disordered superconductor-normal-metal composite *J Phys F: Met Phys* (1987) **17** 447
- 9 Finnemore, D.K., Shelton, R.N., Clem, J.R., McCallum, R.W., Ku, H.C., McCarley, R.E., Chen, S.C., Klavins, P. and Kogan, V. Magnetization of superconducting lanthanum copper oxides *Phys Rev B* (1987) **35** 5319
- 10 Ekin, J.W., Panson, A.J., Braginski, A.I., Janocko, M.A., Hong, M., Kwo, J., Liou, S.H., Capone, II, D.W. and Flandermeyer, B. Transport critical-current characteristics of  $Y_1Ba_2Cu_3O_x$ , in: *High Temperature Superconductors* (Eds Gubser, D.U. and Schluter, M.) Materials Research Society, Pittsburgh, USA (1987) EA-11 223
- 11 Suenaga, M., Ghosh, A., Asano, T., Sabatini, R.L. and Moodenbaugh, A.R. Superconducting properties and microstructures of  $La_{1.85}Sr_{0.15}CuO_4$  and  $YBa_2Cu_3O_x$ , in: *High Temperature Superconductors* (Eds Gubser, D.U. and Schluter, M.) Materials Research Society, Pittsburgh, USA (1987) EA-11 247
- 12 Wenger, L.E. and Chen, J.T. personal communication, Wayne State University, USA (1987)
- 13 Larbalestier, D.C., Daeumling, M., Cai, X., Seuntjens, J., McKinnell, J., Hampshire, D., Lee, P., Meingast, C., Willis, T., Muller, H., Ray, R.D., Dillenburg, R.G., Hellstrom, E.E. and Joynt, R. Experiments concerning the connective nature of superconductivity in  $YBa_2Cu_3O_{7-x}$  *J Appl Phys* (1987) **62** in press
- 14 Clem, J.R. and Kogan, V.G. Theory of the magnetization of granular superconductors: application to high- $T_c$  superconductors *Int Conf Low Temp Physics LT18 Kyoto, Japan Jpn J Appl Phys* (1987) preprint
- 15 Kogan, V.G. and Clem, J.R. Anisotropy effects upon the magnetic

- properties of high- $T_c$  superconductors *Int Conf Low Temp Physics LT18* Kyoto, Japan *Jpn J Appl Phys* (1987) preprint
- 16 Dinger, T.R., Worthington, T.K., Gallagher, W.J. and Sandstrom, R.L. Direct observation of electronic anisotropy in single-crystal  $Y_1Ba_2Cu_3O_{7-x}$  *Phys Rev Lett* (1987) **58** 2687
- 17 Welch, D.O., Suenaga, M. and Asano, T. On the anisotropy of  $H_{c2}$  and the breadth of the resistive transition of polycrystalline  $YBa_2Cu_3O_{7-x}$  in a magnetic field *Phys Rev B* (1987) **36** in press
- 18 Panson, A.J., Braginski, A.I., Gvaler, J.R., Hulm, J.K., Janocko, M.A., Pohl, H.C., Stewart, A.M., Talvacchio, J. and Wagner, G.R. The effect of compositional variation and annealing in oxygen on superconducting properties of  $Y_1Ba_2Cu_3O_{8-y}$  *Phys Rev B* (1987) **35** 8774
- 19 Goldfarb, R.B. and Minervini, J.V. Calibration of a.c. susceptometer for cylindrical specimens *Rev Sci Instrum* (1984) **55** 761
- 20 Chikazumi, S. *Physics of Magnetism* John Wiley, New York, USA (1964) 21
- 21 Oda, Y., Nakada, I., Kohara, T., Fujita, H., Kaneko, T., Toyoda, H., Sakagami, E. and Asayama, K. AC susceptibility of superconducting La-Sr-Cu-O system *Jpn J Appl Phys* (1987) **26** L481
- 22 Maletta, H., Malozemoff, A.P., Cronmeyer, D.C., Tsuei, C.C., Greene, R.L., Bednorz, J.G. and Müller, K.A. Diamagnetic shielding and Meissner effect in the high  $T_c$  superconductor  $Sr_{0.2}La_{1.8}CuO_4$  *Solid State Commun* (1987) **62** 323
- 23 Gallagher, W.J., Sandstrom, R.L., Dinger, T.R., Shaw, T.M. and Chance, D.A. Identification and preparation of single phase 90 K oxide superconductor and structural determination by lattice imaging *Solid State Commun* (1987) **63** 147
- 24 Rao, K.V., Chen, D.-X., Nogues, J., Politis, C., Gallo, C. and Gerber, J.A. Frequency and field dependencies of the a.c. susceptibility: a probe to the microstructure of high  $T_c$  superconducting materials, in *High Temperature Superconductors* (Eds Gubser, D. U. and Schluter, M.) Materials Research Society, Pittsburgh, USA (1987) EA-11 133
- 25 Fetter, A.L. and Hohenberg, P.C. Theory of type II superconductors, in: *Superconductivity* (Ed Parks, R.D.) Marcel Dekker, New York, USA (1969) 843
- 26 Saint-James, D., Thomas, E.J. and Sarma, G. *Type II Superconductivity* Pergamon, Oxford, UK (1969) 28